

**Figure 1. Molecular cell biologic assay of RALD.** (A) Flow cytometric analysis of double-negative T cells. CD8 and CD4 double staining was performed in T-cell receptor- $\alpha\beta$ -expressing cells. (B) Electropherogram showing KRAS G13D mutation in BM-MNCs in case 1 (left panel) and case 2 (right panel). (C) Gene dosage of mutated allele in granulocytes (Gr), T cells (T), and B cells (B). Relative gene dosage was estimated by a mutant allele-specific polymerase chain reaction method in cases 1 and 2 using albumin gene as internal control. (D) Apoptosis assay using activated T cells. Apoptosis percentage was measured by flow cytometry with annexin V staining 24 and 48 hours after IL-2 depletion. (E) Apoptosis percentage was measured 24 hours after addition of anti-FAS CH11 antibody (final 100 ng/mL). (F) Western blotting analysis of Bim expression.

**Case 2**

A 5-month-old girl had a fever and massive hepatosplenomegaly (supplemental Figure 1D). She was initially diagnosed with Evans syndrome based on the presence of hemolytic anemia and autoimmune thrombocytopenia with hyper- $\gamma$ -globulinemia and autoantibodies. Spontaneous colony formation assay and GM-CSF hypersensitivity of BM-MNCs showed positivity. Then, tentative diagnosis of JMML was given, even though she showed no massive monocytosis or increased fetal hemoglobin. Detailed clinical history and laboratory data are provided in supplemental data.

Detailed methods for experiments are described in supplemental data.

**Results and discussion**

Case 1 showed a high likelihood of being a case of ALPS according to the symptoms and clinical data presented (supplemental Table 1), except for number of double-negative T cells, which was only 1.4% of T-cell receptor- $\alpha\beta$  cells (Figure 1A). JMML was also nominated as a disease to be differentiated because remarkable hepatosplenomegaly with thrombocytopenia and moderate monocytosis was

noted. However, no hypersensitivity to GM-CSF as determined by colony formation assay for BM-MNCs (data not shown) or phosphor-STAT5 staining (data not shown) was observed. DNA sequence for JMML-associated genes, such as *NRAS*, *KRAS*, *HRAS*, *PTPN11*, and *CBL*, was determined, and *KRAS* G13D mutation was identified (Figure 1B). The mutation was seen exclusively in the hematopoietic cell lineage, and no mutation was seen in the oral mucosa or nail-derived DNA. Granulocytes, monocytes, T cells, and B cells were all positive for *KRAS* G13D mutation (data not shown). The proportion of mutated cells in each hematopoietic lineage was quantitated by mutation allele-specific quantitative polymerase chain reaction methods, which revealed that mutated allele was almost equally present in granulocytes, T cells, and B cells (Figure 1C). CD34<sup>+</sup> hematopoietic stem cells (HSCs) were also positive for *KRAS* G13D mutation, and 60% of colony-forming units-granulocyte macrophage (CFU-GM) developed from isolated CD34 cells carried the *KRAS* G13D mutation (data not shown). These observations suggest that the mutation occurred at the HSCs level, and HSC consists of wild-type and mutant HSCs.

*NRAS*-mutated type IV ALPS was previously characterized by apoptosis resistance of T cells in IL-2 depletion.<sup>3</sup> Then, activated T cells were subjected to an apoptosis assay by FAS stimulation or IL-2 depletion. Remarkable resistance to IL-2 depletion, but not to FAS-dependent apoptosis (Figure 1D-E), was seen. This was in contrast to T cells from FAS-mutated ALPS type 1a, which showed remarkable resistance to FAS-dependent apoptosis and normal apoptosis induction by IL-2 withdrawal (Figure 1D-E). Western blotting analysis of activated T cells or Epstein-Barr virus-transformed B cells showed reduced expression of Bim (Figure 1F).

In case 2, autoimmune phenotype and hepatosplenomegaly were remarkable, as shown in Supplemental data. The patient was initially diagnosed as Evans syndrome based on the presence of hemolytic anemia and autoimmune thrombocytopenia. Double-negative T cells were 1.1% of T-cell receptor- $\alpha\beta$  cells in the peripheral blood, which did not meet with the criteria of ALPS. Although spontaneous colony formation was shown in peripheral blood- and BM-MNCs, and GM-CSF hypersensitivity was demonstrated in BM-MNCs derived CD34<sup>+</sup> cell (supplemental Table 2), she showed no massive monocytosis or increased fetal hemoglobin. Thus, the diagnosis was less likely to be ALPS or JMML. DNA sequencing of JMML-related genes, such as *NRAS*, *KRAS*, *HRAS*, *PTPN11*, and *CBL*, identified somatic, but not germline, *KRAS* G13D mutation (Figure 1B). *KRAS* G13D mutation was detected in granulocytes and T cells. Mutation was not identified in B cells by conventional DNA sequencing (data not shown). Mutant allele-specific quantitative polymerase chain reaction revealed that mutated allele was almost equally present in granulocytes and T cells, but barely in B cells (Figure 1C). Activated T cells showed resistance to IL-2 depletion but not to FAS-dependent apoptosis (Figure 1D-E).

Both of our cases were characterized by strong autoimmunity, immune cytopenia, and lymphadenopathy or hepatosplenomegaly with partial similarity with ALPS or JMML. However, they did not meet with the well-defined diagnostic criteria of ALPS<sup>2</sup> or JMML.<sup>6</sup> It is interesting that case 2 presented GM-CSF hypersensitivity, which is one of the hallmarks of JMML. Given the strict clinical and laboratory criteria of JMML and ALPS, our 2 cases should be defined as a new disease entity, such as RAS-associated ALPS-like disease (RALD). Recently

defined *NRAS*-mutated ALPS type IV may also be included in a similar disease entity.

There are several cases of JMML reported simultaneously having clinical and laboratory findings compatible with autoimmune disease.<sup>8,9</sup> Autoimmune syndromes are occasionally seen in patients with myelodysplastic syndromes, including chronic myelomonocytic leukemia.<sup>10</sup> These previous findings may suggest a close relationship of autoimmune disease and JMML. Because *KRAS* G13D has been identified in JMML,<sup>11-13</sup> it is tempting to speculate that *KRAS* G13D mutation is involved in JMML as well as RALD. In JMML, erythroid cells reportedly carry mutant RAS, whereas B- and T-cell involvement was variable.<sup>13</sup> In both of our cases, myeloid cells and T cells carried mutant RAS, whereas B cells were affected variably. These findings would support a hypothesis that the clinical and hematologic features are related to the differentiation stages of HSCs where RAS mutation is acquired. JMML-like myelomonocytic proliferation may predict an involvement of RAS mutation in myeloid stem/precursor cell level, whereas ALPS-like phenotype may predict that of stem/precursor cells of lymphoid lineage, especially of T cells. Under the light of subtle differences between the 2 cases presented, their hematologic and clinical features may reflect the characteristics of the stem cell level where *KRAS* mutation is acquired. Involvement of the precursors with higher propensity toward lymphoid lineage may lead to autoimmune phenotypes, whereas involvement of those with propensity toward the myeloid lineage may lead to GM-CSF hypersensitivity while still sharing some overlapping autoimmune characteristics.

One may argue from the other viewpoints with regard to the clinicopathologic features of these disorders. First, transformation in fetal HSCs might be obligatory for the development of JMML<sup>14</sup> and, in HSCs later in life, may not have the same consequences. Second, certain *KRAS* mutations may be more potent than others. Codon 13 mutations are generally less deleterious biochemically than codon 12 substitutions, and patients with JMML with codon 13 mutations have been reported to show spontaneous hematologic improvement.<sup>12,15</sup> Thus, further studies are needed to reveal in-depth clinicopathologic characteristics in this type of lymphomyeloproliferative disorder.

*KRAS* mutation may initiate the oncogenic pathway as one of the first genetic hits but is insufficient to cause frank malignancy by itself.<sup>16,17</sup> Considering recent findings that additional mutations of the genes involved in DNA repair, cell cycle arrest, and apoptosis are required for full malignant transformation, one can argue that RALD patients will also develop malignancies during the course of the disease. Occasional association of myeloid blast crisis in JMML and that of lymphoid malignancies in ALPS will support this notion. Thus, the 2 patients are now being followed up carefully. It was recently revealed that half of the patients diagnosed with Evans syndrome, an autoimmune disease presenting with hemolytic anemia and thrombocytopenia, met the criteria for ALPS diagnosis.<sup>18,19</sup> In this study, FAS-mediated apoptosis analysis was used for the screening. Considering the cases we presented, it will be intriguing to reevaluate Evans syndrome by IL-2 depletion-dependent apoptosis assay focusing on the overlapping autoimmunity with RALD.

## Acknowledgments

This work was supported by the Ministry of Education, Science, and Culture of Japan (Grant-in-Aid 20390302; S.M.) and the

Ministry of Health, Labor and Welfare of Japan (Grant-in-Aid for Cancer Research 20-4 and 19-9; S.M., Masatoshi Takagi).

S.K., Y.K., and A.T. supervised clinical and immunologic experiments or coordinated clinical information.

Conflict-of-interest disclosure: The authors declare no competing financial interests.

Correspondence: Masatoshi Takagi, Department of Pediatrics and Developmental Biology, Graduate School of Medicine, Tokyo Medical and Dental University, 1-5-45 Yushima, Bunkyo-ku, Tokyo, 113-8519, Japan; e-mail: m.takagi.ped@tmd.ac.jp; and Shuki Mizutani, Department of Pediatrics and Developmental Biology, Graduate School of Medicine, Tokyo Medical and Dental University, 1-5-45 Yushima, Bunkyo-ku, Tokyo, 113-8519, Japan; e-mail: smizutani.ped@tmd.ac.jp.

## Authorship

Contribution: Masatoshi Takagi and S.M. designed entire experiments and wrote the manuscript; K.S., N.M., and Mari Takagi treated patients and designed clinical laboratory test; J.P. performed experiments described in Figure 1B-F; K.M., H.M., and S.D. performed colony and mutational analysis; and M.N., T.M., K.K.,

## References

- Fisher GH, Rosenberg FJ, Straus SE, et al. Dominant interfering Fas gene mutations impair apoptosis in a human autoimmune lymphoproliferative syndrome. *Cell*. 1995;81(6):935-946.
- Teachey DT, Seif AE, Grupp SA. Advances in the management and understanding of autoimmune lymphoproliferative syndrome (ALPS). *Br J Haematol*. 2010;148(2):205-216.
- Oliveira JB, Bidere N, Niemela JE, et al. NRAS mutation causes a human autoimmune lymphoproliferative syndrome. *Proc Natl Acad Sci U S A*. 2007;104(21):8953-8958.
- Oliveira J, Bleesing J, Dianzani U, et al. Revised diagnostic criteria and classification for the autoimmune lymphoproliferative syndrome (ALPS): report from the 2009 NIH International Workshop. *Blood*. 2010;116(14):e35-e40.
- Miyauchi J, Asada M, Sasaki M, Tsunematsu Y, Kojima S, Mizutani S. Mutations of the N-ras gene in juvenile chronic myelogenous leukemia. *Blood*. 1994;83(8):2248-2254.
- Emanuel PD. Juvenile myelomonocytic leukemia and chronic myelomonocytic leukemia. *Leukemia*. 2008;22(7):1335-1342.
- Aoki Y, Niihori T, Narumi Y, Kure S, Matsubara Y. The RAS/MAPK syndromes: novel roles of the RAS pathway in human genetic disorders. *Hum Mutat*. 2008;29(8):992-1006.
- Kitahara M, Koike K, Kurokawa Y, et al. Lupus nephritis in juvenile myelomonocytic leukemia. *Clin Nephrol*. 1999;51(5):314-318.
- Oliver JW, Farnsworth B, Tonk VS. Juvenile myelomonocytic leukemia in a child with Crohn disease. *Cancer Genet Cytogenet*. 2006;167(1):70-73.
- Saif MW, Hopkins JL, Gore SD. Autoimmune phenomena in patients with myelodysplastic syndromes and chronic myelomonocytic leukemia. *Leuk Lymphoma*. 2002;43(11):2083-2092.
- Flotho C, Kratz CP, Bergstrasser E, et al. Genotype-phenotype correlation in cases of juvenile myelomonocytic leukemia with clonal RAS mutations. *Blood*. 2008;111(2):966-967.
- Matsuda K, Shimada A, Yoshida N, et al. Spontaneous improvement of hematologic abnormalities in patients having juvenile myelomonocytic leukemia with specific RAS mutations. *Blood*. 2007;109(12):5477-5480.
- Flotho C, Valcamonica S, Mach-Pascual S, et al. RAS mutations and clonality analysis in children with juvenile myelomonocytic leukemia (JMML). *Leukemia*. 1999;13(1):32-37.
- Matsuda K, Sakashita K, Taira C, et al. Quantitative assessment of PTPN11 or RAS mutations at the neonatal period and during the clinical course in patients with juvenile myelomonocytic leukemia. *Br J Haematol*. 2010;148(4):593-599.
- Imamura M, Imai C, Takachi T, Nemoto T, Tanaka A, Uchiyama M. Juvenile myelomonocytic leukemia with less aggressive clinical course and KRAS mutation. *Pediatr Blood Cancer*. 2008;51(4):569.
- Zhang J, Wang J, Liu Y, et al. Oncogenic Kras-induced leukemogenesis: hematopoietic stem cells as the initial target and lineage-specific progenitors as the potential targets for final leukemic transformation. *Blood*. 2009;113(6):1304-1314.
- Sabnis AJ, Cheung LS, Dail M, et al. Oncogenic Kras initiates leukemia in hematopoietic stem cells. *PLoS Biol*. 2009;7(3):0537-0548.
- Teachey DT, Manno CS, Axsom KM, et al. Unmasking Evans syndrome: T-cell phenotype and apoptotic response reveal autoimmune lymphoproliferative syndrome (ALPS). *Blood*. 2005;105(6):2443-2448.
- Seif AE, Manno CS, Sheen C, Grupp SA, Teachey DT. Identifying autoimmune lymphoproliferative syndrome in children with Evans syndrome: a multi-institutional study. *Blood*. 2010;115(11):2142-2145.



# NIH Public Access

## Author Manuscript

*Arthritis Rheum.* Author manuscript; available in PMC 2012 November 15.

Published in final edited form as:

*Arthritis Rheum.* 2011 November ; 63(11): 3625–3632. doi:10.1002/art.30512.

## High Incidence of *NLRP3* Somatic Mosaicism in Patients With Chronic Infantile Neurologic, Cutaneous, Articular Syndrome: Results of an International Multicenter Collaborative Study

Naoko Tanaka<sup>1,†</sup>, Kazushi Izawa<sup>1,†</sup>, Megumu K. Saito<sup>2</sup>, Mio Sakuma<sup>3</sup>, Koichi Oshima<sup>4</sup>, Osamu Ohara<sup>4,\*</sup>, Ryuta Nishikomori<sup>1,\*</sup>, Takeshi Morimoto<sup>3</sup>, Naotomo Kambe<sup>5</sup>, Raphaela Goldbach-Mansky<sup>6,‡</sup>, Ivona Aksentijevich<sup>6</sup>, Geneviève de Saint Basile<sup>7</sup>, Bénédicte Neven<sup>8</sup>, Mariëlle van Gijn<sup>9</sup>, Joost Frenkel<sup>9</sup>, Juan I. Aróstegui<sup>10</sup>, Jordi Yagüe<sup>10</sup>, Rosa Merino<sup>11</sup>, Mercedes Ibañez<sup>12</sup>, Alessandra Pontillo<sup>13</sup>, Hidetoshi Takada<sup>14</sup>, Tomoyuki Imagawa<sup>15</sup>, Tomoki Kawai<sup>1</sup>, Takahiro Yasumi<sup>1</sup>, Tatsutoshi Nakahata<sup>2</sup>, and Toshio Heike<sup>1</sup>

<sup>1</sup>Kyoto University Graduate School of Medicine, Kyoto, Japan <sup>2</sup>Center for iPS Cell Research and Application, Kyoto, Japan <sup>3</sup>Kyoto University, Kyoto, Japan <sup>4</sup>RIKEN Yokohama Institute, Yokohama, Kanagawa, and Kazusa DNA Research Institute, Kisarazu, Chiba, Japan <sup>5</sup>Chiba University Graduate School of Medicine, Chiba, Japan <sup>6</sup>National Institute of Arthritis and Musculoskeletal and Skin Diseases, NIH, Bethesda, Maryland <sup>7</sup>Paris Descartes University and INSERM U 768, Paris, France <sup>8</sup>Necker Hospital for Sick Children, AP-HP, Paris, France <sup>9</sup>University Medical Centre Utrecht, Utrecht, The Netherlands <sup>10</sup>Hospital Clínic, Barcelona, Spain <sup>11</sup>Hospital La Paz, Madrid, Spain <sup>12</sup>Hospital Niño Jesús, Madrid, Spain <sup>13</sup>IRCCS Burlo Garofalo, Trieste, Italy <sup>14</sup>Kyushu University Graduate School of Medical Sciences, Fukuoka, Japan <sup>15</sup>Yokohama City University School of Medicine, Yokohama, Kanagawa, Japan

### Abstract

**Objective**—Chronic infantile neurologic, cutaneous, articular (CINCA) syndrome, also known as neonatal-onset multisystem inflammatory disease (NOMID), is a dominantly inherited systemic autoinflammatory disease. Although heterozygous germline gain-of-function *NLRP3* mutations are a known cause of this disease, conventional genetic analyses fail to detect disease-causing mutations in ~40% of patients. Since somatic *NLRP3* mosaicism has been detected in several mutation-negative NOMID/CINCA syndrome patients, we undertook this study to determine the precise contribution of somatic *NLRP3* mosaicism to the etiology of NOMID/CINCA syndrome.

**Methods**—An international case-control study was performed to detect somatic *NLRP3* mosaicism in NOMID/CINCA syndrome patients who had shown no mutation during conventional sequencing. Subcloning and sequencing of *NLRP3* was performed in these mutation-

\*Osamu Ohara (ohara@kazusa.or.jp), Ryuta Nishikomori (rnishiko@kuhp.kyoto-u.ac.jp), Department of Human Genome Research, Kazusa DNA Research Institute, 2-6-7 Kazusakamataru Kisarazu, Chiba 292-0818, Japan.

†Drs. Tanaka and Izawa contributed equally to this work.

‡Dr. Goldbach-Mansky has served as an expert witness on behalf of Biovitrum, Novartis, and Regeneron.

#### Author Contributions

All authors were involved in drafting the article or revising it critically for important intellectual content, and all authors approved the final version to be published. Drs. Ohara and Nishikomori had full access to all of the data in the study and take responsibility for the integrity of the data and the accuracy of the data analysis.

**Study conception and design.** Saito, Ohara, Nishikomori, Kambe

**Acquisition of data.** Tanaka, Izawa, Saito, Oshima, Ohara, Nishikomori, Goldbach-Mansky, Aksentijevich, de Saint Basile, Neven, van Gijn, Frenkel, Aróstegui, Yagüe, Merino, Ibañez, Pontillo, Takada, Imagawa.

**Analysis and interpretation of data.** Sakuma, Morimoto, Kawai, Yasumi, Nakahata, Heike.

negative NOMID/CINCA syndrome patients and their healthy relatives. Clinical features were analyzed to identify potential genotype–phenotype associations.

**Results**—Somatic *NLRP3* mosaicism was identified in 18 of the 26 patients (69.2%). Estimates of the level of mosaicism ranged from 4.2% to 35.8% (mean  $\pm$  SD 12.1  $\pm$  7.9%). Mosaicism was not detected in any of the 19 healthy relatives (18 of 26 patients versus 0 of 19 relatives;  $P < 0.0001$ ). In vitro functional assays indicated that the detected somatic *NLRP3* mutations had disease-causing functional effects. No differences in *NLRP3* mosaicism were detected between different cell lineages. Among nondescript clinical features, a lower incidence of mental retardation was noted in patients with somatic mosaicism. Genotype-matched comparison confirmed that patients with somatic *NLRP3* mosaicism presented with milder neurologic symptoms.

**Conclusion**—Somatic *NLRP3* mutations were identified in 69.2% of patients with mutation-negative NOMID/CINCA syndrome. This indicates that somatic *NLRP3* mosaicism is a major cause of NOMID/CINCA syndrome.

Chronic infantile neurologic, cutaneous, articular (CINCA) syndrome (MIM no. #607715), also known as neonatal-onset multisystem inflammatory disease (NOMID), is a dominantly-inherited autoinflammatory disease that is characterized by neonatal onset and the triad of urticarial-like skin rash, neurologic manifestations, and arthritis/arthropathy. Patients often experience recurrent fever and systemic inflammation. NOMID/CINCA syndrome is the most severe clinical phenotype of the cryopyrin-associated periodic syndromes (CAPS) that also include the 2 less severe but phenotypically similar syndromes familial cold autoinflammatory syndrome (FCAS; MIM no. #120100) and Muckle-Wells syndrome (MIM no. #191900). CAPS are caused by mutations in the *NLRP3* gene, which is a member of the nucleotide-binding oligomerization domain–like receptor (NLR) family of the innate immune system (1, 2).

NLRP3 is an intracellular “sensor” of danger signals arising from cellular insults, such as infection, tissue damage, and metabolic deregulation, and it has been highly conserved throughout evolution. NLRP3 associates with ASC and procaspase 1 to constitute a large multiprotein complex termed the NLRP3 inflammasome. When activated, the NLRP3 inflammasome converts the biologically inactive procaspase 1 into active caspase 1. Caspase 1 produces the cytokines interleukin-1 $\beta$  (IL-1 $\beta$ ) and IL-18, which are mainly involved in the inflammatory response (3). Available research suggests that mutated *NLRP3* induces autoactivation of the NLRP3 inflammasome in CAPS patients, resulting in an uncontrolled overproduction of IL-1 $\beta$ .

Most CAPS patients carry heterozygous germline missense mutations in the *NLRP3* coding region (“mutation-positive” patients) (4, 5). More than 80 different disease-causing mutations have been reported to date (6). However, ~40% of clinically diagnosed NOMID/CINCA syndrome patients show no heterozygous germline *NLRP3* mutation during conventional Sanger-sequencing-based genetic analyses (“mutation-negative” patients). Comparisons of NOMID/CINCA syndrome patients with and without heterozygous germline *NLRP3* mutations have revealed no differences in clinical features or response to treatment (4, 7).

In a previous study, we identified a high incidence of somatic *NLRP3* mosaicism in “mutation-negative” NOMID/CINCA syndrome patients in Japan (8). We therefore hypothesized that somatic *NLRP3* mosaicism may be implicated in the etiology of the disorder, although its precise contribution remains unclear. The aim of the present study was to evaluate both the frequency of *NLRP3* somatic mosaicism in NOMID/CINCA syndrome

patients and the association between somatic mosaicism and clinical phenotype using an international cohort of mutation-negative NOMID/CINCA syndrome patients.

## Patients and Methods

### Study design and participants

International collaborators were contacted to identify mutation-negative NOMID/CINCA syndrome cases. A total of 20 DNA samples were received from 4 centers: France (n = 6), The Netherlands (n = 4), Spain (n = 3), and the US (n = 7). DNA samples had been extracted from peripheral blood mononuclear cells or whole blood. All 20 samples had been subjected to conventional sequencing, and no *NLRP3* mutations had been identified. In each case, the accuracy of the clinical diagnosis had been confirmed according to the diagnostic criteria (7). The 6 previously reported Japanese cases and 1 Spanish case with *NLRP3* somatic mosaicism were also included (8, 9). DNA samples were also collected from 19 healthy relatives of 8 patients (8 from France, 5 from Japan, 2 from Spain, and 4 from the US) to evaluate the causality of somatic *NLRP3* mosaicism in a case-control manner, since the clinical features may be modified by genetic and environmental factors.

Written informed consent for *NLRP3* gene analysis was obtained from all patients and controls. The study was approved by the Institutional Review Board of the Kyoto University Graduate School of Medicine and was conducted in accordance with the Declaration of Helsinki.

### Data collection

**Demographic and clinical data**—The clinicians responsible for each mutation-negative NOMID/CINCA syndrome patient completed a questionnaire to document characteristics such as age, sex, race, symptoms, clinical findings, clinical course, and prognosis. No clinical data were obtained from the healthy controls.

**Investigation of *NLRP3* gene mosaicism**—Disease-causing mutations in NOMID/CINCA syndrome patients have only been reported in exons 3, 4, and 6 of *NLRP3* (6). Thus, the present sequencing was focused on a search for somatic mosaicism of these 3 exons and their flanking intronic regions. After amplifying these genomic regions with the proofreading polymerase chain reaction (PCR) enzyme KOD-Plus polymerase (Toyobo) and dA addition with an LA *Taq* polymerase (Takara Bio), the amplicons were subcloned into pCR2.1-TOPO vector (Invitrogen). Ninety-six clones were selected at random for each amplicon. The subcloned amplicons were retrieved by PCR with LA *Taq* polymerase. They were then treated with ExoSAP-IT (USB) and proteinase K (Promega) prior to direct sequencing. The cloned exons were sequenced at the Kazusa DNA Research Institute using a BigDye Terminator kit (version 3.1) and an ABI 3730 DNA sequencer (Life Technologies). Mosaicism was indicated by the detection of >2 subclones carrying the same base variation at the same position in 96 clones.

To purify leukocyte subpopulations, freshly drawn whole blood was separated using sequential dextran and Ficoll-Hypaque density-gradient centrifugation methods. Cell sorting to select T cells, B cells, and monocytes was performed with an AutoMACS Pro Separator (Miltenyi Biotec) or a FACSVantage System (BD Biosciences), as described elsewhere (8, 9). The purity of each cell lineage was >90%. The level of mosaicism was determined by sequencing each source of genomic DNA from 80 clones.

**Plasmids and cell lines**—To determine whether the identified *NLRP3* mutants cause disease, experiments for assessing 2 pathologic functions were performed as described

elsewhere (8). Briefly, ASC-dependent NF- $\kappa$ B activation was performed by a dual-luciferase reporter assay in HEK 293FT cells transfected with NLRP3 mutants. Transfection-induced cell death in the human monocytic cell line THP-1 was performed by transfecting green fluorescent protein–fused mutant NLRP3 into THP-1 cells and then measuring the dead cells with 7-aminoactinomycin D.

### Statistical analysis

The study was designed to detect mosaicism at a 5% allele frequency with >95% possibility. To satisfy this condition, it was necessary to sequence at least 93 clones per patient. The following calculation was used to estimate the number of clones that had to be sequenced:  $P = 1 - (1 - 0.05)^n - n(0.05)(1 - 0.05)^{n-1}$  ( $n = 93$ ,  $P = 0.956$ ). The study was designed to analyze 96 PCR-fragment clones from each patient. The error rate of the PCR reactions was estimated using a proofreading KOD-Plus enzyme. We analyzed a plasmid vector carrying a normal *NLRP3* exon 3, in which 2 distinct errors were detected by sequencing 91 clones. The calculated error rate for this result was 1/87,451 ( $2/[1,922 \text{ bp} \times 91 \text{ clones}]$ ). Thus, the probability was negligible that the same errors would be detected more than twice in 96 clones from 1 patient.

To calculate the sample size, we calculated the prevalence of somatic mosaicism among mutation-negative NOMID/CINCA syndrome patients. Eight cases of somatic mosaicism were identified among 15 mutation-negative NOMID/CINCA syndrome patients who were subsequently analyzed by the subcloning method described above. It was assumed that the maximum number of possible somatic mosaicism cases among family controls was 1. On the basis of these data and this assumption, it was calculated that 19 controls were required to ensure a 2-sided alpha level of 0.05 and a power of 0.8.

Continuous variables are presented as the mean  $\pm$  SD or as the median and interquartile range. Categorical variables are presented as numbers and ratios (with percentages). To compare clinical data between patients with and patients without mosaicism, the Wilcoxon rank sum test was used for continuous variables and Fisher's exact test was used for categorical variables. Fisher's exact test was used to compare the difference in mosaicism ratio between cases and controls. The chi-square test was used to compare the difference in the level of mosaicism between different sources of genomic DNA from each patient.

## Results

### Somatic *NLRP3* mosaicism in mutation-negative NOMID/CINCA syndrome patients

A heterozygous germline *NLRP3* mutation was detected in 1 of the 27 samples, and this was therefore excluded from the analyses. For each patient, 96 clones were selected at random for each amplicon. These were then sequenced. *NLRP3* mosaicism was detected in 18 of 26 patients (69.2%), and the level of allelic mosaicism ranged from 4.2% to 35.8% (mean  $\pm$  SD  $12.1 \pm 7.9\%$ ; median 10.2%) (Table 1). Seven of the detected *NLRP3* mutations were novel (p.G307S, p.K355N, p.M406V, p.T433I, p.F566L, p.E567K, and p.K568N). The remaining mutations have been reported previously in NOMID/CINCA syndrome patients as disease-causing heterozygous germline mutations (p.L264F, p.D303H, p.G307V, p.A439P, p.Y570C, and p.G755R). Each of the 3 *NLRP3* mutations, p.F566L, p.E567K, and p.G755R, was detected in 2 unrelated patients. *NLRP3* mutation p.D303H was detected in 3 unrelated patients.

### Analyses in family controls

To validate the clinical relevance of the *NLRP3* mosaicism identified in mutation-negative NOMID/CINCA syndrome patients, samples from 19 healthy relatives were investigated.

No somatic mosaicism was detected in any of these samples. The  $P$  value from the comparison of cases and controls (18 of 26 versus 0 of 19) was statistically significant ( $P < 0.0001$ ).

### Functional effects of the identified somatic *NLRP3* mutations

Since disease-causing heterozygous germline mutations in *NLRP3* have been implicated in necrosis-like programmed cell death and ASC-dependent NF- $\kappa$ B activation (8), experiments were performed to determine whether the mutations identified in patients with somatic mosaicism showed the same effects. All of the identified mutations induced both THP-1 cell death (Figure 1A) and ASC-dependent NF- $\kappa$ B activation (Figure 1B). The in vitro effects of these novel mutations were similar to or even more pronounced than those of previously reported *NLRP3* mutations. This strongly suggests that all mutations showing somatic mosaicism have pathogenic effects, including the novel mutations identified in the present study.

### Mutation frequency of *NLRP3* among various cell lineages and 1 tissue type

To explore the origin of the *NLRP3* mosaicism, mutational frequency was evaluated in various cell lineages and 1 tissue type from 4 Japanese patients with *NLRP3* somatic mosaicism. In each patient, the same mutations were found in all of the cell lineages investigated (neutrophils, monocytes, T cells, B cells) and in the buccal mucosa tissue, and no significant difference in mutation frequency was observed between these sources (Table 2).

### Phenotype–genotype analysis

Given the previously reported genotype–phenotype association between the *NLRP3* gene and CAPS, the clinical characteristics of NOMID/CINCA syndrome patients with somatic *NLRP3* mutations were compared with those of patients from previous reports who had the same *NLRP3* mutations but with heterozygous germline status (1, 4, 10-13) (Figure 2) (further information is available at Supplemental Tables 1 and 2. All of the patients in these 2 groups had an early onset of the disease, fever, and urticarial rash. The presence of arthritis, bony overgrowth, contractures, hearing loss, and seizure varied in each group of patients, and no significant difference was detected. However, whereas most patients with heterozygous germline *NLRP3* mutations presented with mental retardation, this was not the case for patients with somatic *NLRP3* mosaicism. A comparison was also made between the clinical data from patients with somatic *NLRP3* mosaicism and the data from patients with neither germline nor somatic *NLRP3* mutations. Again, a lower incidence of mental retardation was observed in patients with somatic *NLRP3* mosaicism ( $P = 0.03$ ). No other significant differences were detected (Table 3) (further information is available at Supplemental Tables 1 and 2.

## Discussion

The present international multicenter study investigated 26 NOMID/CINCA syndrome patients who were mutation negative according to conventional sequencing along with 19 family controls to determine whether low-level mosaicism is a disease-causing genetic mechanism. Following our first report of low-level somatic mosaicism in a NOMID/CINCA syndrome patient (14), we reported a new method of detecting low-level *NLRP3* mosaicism, in which lipopolysaccharide (LPS) induced cell death specifically in *NLRP3* mutation–positive monocytes (8). However, this method requires fresh live monocytes, special equipment such as a cell sorter, and experience in its use due to the rapid time course of LPS-induced necrotic monocytic death. For these reasons, application of this method was not feasible in an international collaborative study. We therefore opted to use genomic



DNA, since it is easier to handle and can be stored and shipped. Based on our previous study in Japanese patients showing that the frequency of mutant alleles could be <5%, we designed a subcloning and Sanger-sequencing strategy that could detect this very low allelic mutation frequency.

Presuming that the present cohort is representative of the 40% of NOMID/CINCA syndrome patients who are mutation negative according to conventional sequencing, the results suggest that ~28% of all NOMID/CINCA syndrome patients may carry somatic *NLRP3* mosaicism. CAPS patients present with a continuous spectrum of symptoms, and a degree of genotypic overlap is observed between disease subtypes. Although the present study focused on the most severe NOMID/CINCA syndrome phenotype, it is possible that somatic *NLRP3* mosaicism may also occur in milder forms of CAPS. The presence of somatic mosaicism should also be investigated in patients with other dominantly inherited autoinflammatory diseases caused by gain-of-function mutations and who are mutation negative according to conventional sequencing.

Among the 18 patients with somatic *NLRP3* mosaicism, we found 6 mutations that have previously been identified in NOMID/CINCA syndrome patients as heterozygous germline mutations. We also identified 7 novel mutations, which were confirmed as being functionally active and presumably pathogenic. Functional in vitro assays showed that these novel mutations had greater disease-causing capacity than the previously described mutations. This suggests that the novel mutations may be deleterious and unrecognized if inherited as heterozygous germline mutations.

The present study also addressed the important question of how somatic *NLRP3* mosaicism modifies clinical presentation. Although no statistically significant differences in age at disease onset, skin symptoms, joint involvement, or response to IL-1 blockade were detected, milder neurologic involvement was observed in patients with somatic mosaicism. Comparisons with NOMID/CINCA syndrome patients carrying the same *NLRP3* mutations but with heterozygous germline status made this tendency more prominent. Although the level of somatic mosaicism in blood leukocytes was relatively low, it remains unclear how these low-level mutations influence clinical presentation, including disease severity. One interesting hypothesis is that the difference in the severity of neurologic manifestations is a function of the level of mosaicism. For ethical and technical reasons, it was not possible to evaluate the level of mosaicism in central nervous system (CNS) cells or glial cells in the present study, and this therefore awaits investigation in future studies.

The mechanism through which *NLRP3* somatic mosaicism occurs also requires elucidation. The present study demonstrated that similar proportions of neutrophils, T cells, B cells, monocytes, and buccal cells carried the mutated allele. Therefore, the mutation leading to mosaicism must have arisen before the pluripotent stem cells committed to hematopoietic progenitor stem cells or ectoderm-derived nonhematopoietic cells. Several mechanisms for mosaicism have been proposed, including chimerism due to cell fusion with an aborted dizygotic twin and a mutational event during early embryogenesis (15). The latter mechanism is more likely in the present cohort, since mosaicism at similar frequency was detected in several cell types. To verify the hypothesis of a mutational event during embryogenesis, and to determine the point at which this occurred, it would be helpful to analyze other tissues. However, obtaining such tissues from patients may be ethically problematic.

Approximately 12% of the patients in the present cohort carried neither germline nor somatic *NLRP3* mutations and may therefore be considered to be genuinely mutation negative. However, it is possible that these patients have *NLRP3* mutations that have been

overlooked. A recent report described a mutation in the 5'-untranslated region of *NLRP3* in a patient with FCAS (16), although it remains unclear how this noncoding mutation causes disease. Another possibility is that an extremely low frequency of *NLRP3* mosaicism may have been missed. The subcloning and Sanger-sequencing strategy used in this study set the detection limit of mosaicism at 5%. Considering the range of *NLRP3* mosaicism detected (4.2–35.8%), the median (10.2%), and the identification of 2 patients with <5% mosaicism, it is indeed likely that patients with an even lower level of *NLRP3* mosaicism may have been overlooked. Recent advances in next-generation DNA sequencing technology may resolve this technical problem, although the associated error rate could be problematic. Another possibility is that *NLRP3* mutations were present in uninvestigated cell lineages, such as those from CNS tissue, bone tissue, or skin. Future studies of NOMID/CINCA syndrome should investigate these tissues while searching for mutations in other genes.

In conclusion, the present study has clearly demonstrated that a significant proportion of NOMID/CINCA syndrome patients who were mutation negative according to conventional sequencing carried somatic *NLRP3* mutations with a variable degree of mosaicism. Clinicians should therefore consider somatic mosaicism as a possible cause of disease in mutation-negative NOMID/CINCA syndrome patients and implement appropriate therapy. The early diagnosis of NOMID/CINCA syndrome and prompt initiation of therapy would improve clinical outcome. Further goals in this research field are the refinement of genetic screening and the verification of the functional consequences of all detected somatic mutations. Systematic screening for somatic mosaicism will provide new insights into the etiology of human disease.

## Supplementary Material

Refer to Web version on PubMed Central for supplementary material.

## Acknowledgments

We thank all patients and their relatives for participating in the study. We are grateful to Yuki Takaoka at the Department of Pediatrics, Kyoto University Graduate School of Medicine and Seiko Watanabe at the Department of Human Genome Research, Kazusa DNA Research Institute for their technical assistance.

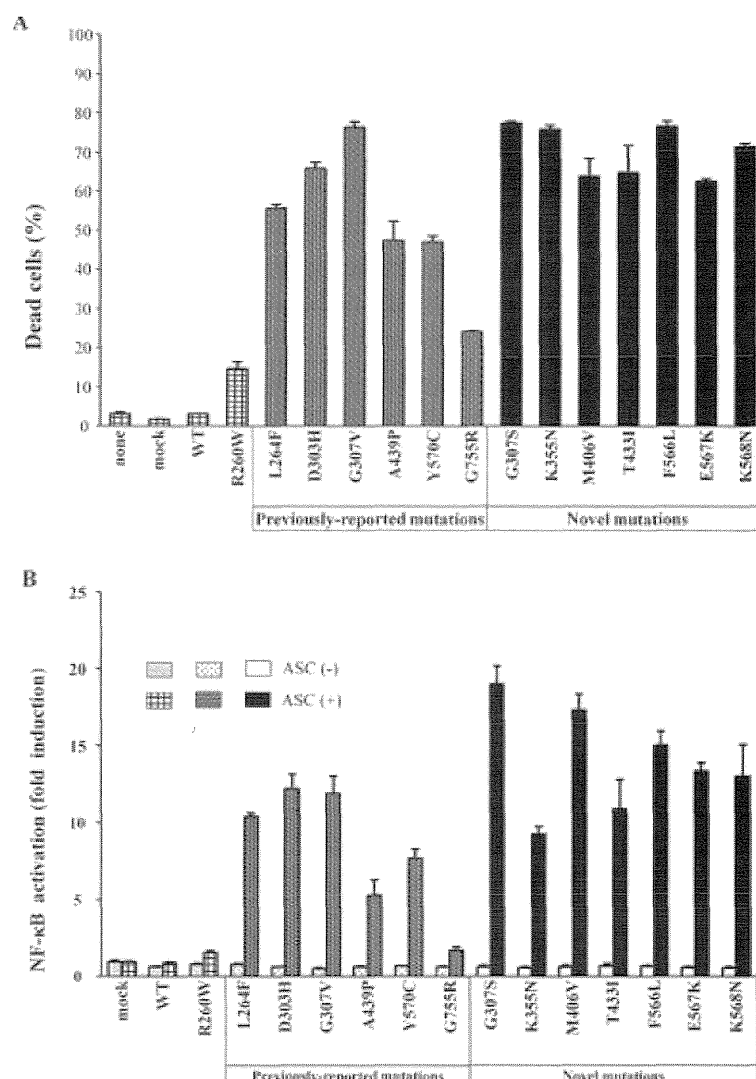
### Role of the Study Sponsor

Mitsubishi Pharma Research Foundation supported the data collection for this study, approved the contents of the manuscript, and agreed to submit the manuscript for publication.

## References

1. Neven B, Callebaut I, Prieur AM, Feldmann J, Bodemer C, Lepore L, et al. Molecular basis of the spectral expression of CIAS1 mutations associated with phagocytic cell-mediated autoinflammatory disorders CINCA/NOMID, MWS, and FCU. *Blood*. 2004; 103:2809–15. [PubMed: 14630794]
2. Stojanov S, Kastner DL. Familial autoinflammatory diseases: genetics, pathogenesis and treatment. *Curr Opin Rheumatol*. 2005; 17:586–99. [PubMed: 16093838]
3. Schroder K, Zhou R, Tschopp J. The NLRP3 inflammasome: a sensor for metabolic danger? *Science*. 2010; 327:296–300. [PubMed: 20075245]
4. Aksentijevich I, Nowak M, Mallah M, Chae JJ, Watford WT, Hofmann SR, et al. De novo CIAS1 mutations, cytokine activation, and evidence for genetic heterogeneity in patients with neonatal-onset multisystem inflammatory disease (NOMID): a new member of the expanding family of pyrin-associated autoinflammatory diseases. *Arthritis Rheum*. 2002; 46:3340–8. [PubMed: 12483741]

5. Hoffman HM, Mueller JL, Broide DH, Wanderer AA, Kolodner RD. Mutation of a new gene encoding a putative pyrin-like protein causes familial cold autoinflammatory syndrome and Muckle-Wells syndrome. *Nat Genet.* 2001; 29:301–5. [PubMed: 11687797]
6. Milhavel F, Cuisset L, Hoffman HM, Slim R, El-Shanti H, Aksentijevich I, et al. The Infevers autoinflammatory mutation online registry: update with new genes and functions. *Hum Mutat.* 2008; 29:803–8. [PubMed: 18409191]
7. Goldbach-Mansky R, Dailey NJ, Canna SW, Gelabert A, Jones J, Rubin BI, et al. Neonatal-onset multisystem inflammatory disease responsive to interleukin-1 $\beta$  inhibition. *N Engl J Med.* 2006; 355:581–92. [PubMed: 16899778]
8. Saito M, Nishikomori R, Kambe N, Fujisawa A, Tanizaki H, Takeichi K, et al. Disease-associated CIAS1 mutations induce monocyte death, revealing low-level mosaicism in mutation-negative cryopyrin-associated periodic syndrome patients. *Blood.* 2008; 111:2132–41. [PubMed: 18063752]
9. Arostegui JI, Lopez Saldana MD, Pascal M, Clemente D, Aymerich M, Balaguer F, et al. A somatic NLRP3 mutation as a cause of a sporadic case of chronic infantile neurologic, cutaneous, articular syndrome/neonatal-onset multisystem inflammatory disease: novel evidence of the role of low-level mosaicism as the pathophysiologic mechanism underlying Mendelian inherited diseases. *Arthritis Rheum.* 2010; 62:1158–66. [PubMed: 20131270]
10. Rosen-Wolff A, Quietzsch J, Schroder H, Lehmann R, Gahr M, Roesler J. Two German CINCA (NOMID) patients with different clinical severity and response to anti-inflammatory treatment. *Eur J Haematol.* 2003; 71:215–9. [PubMed: 12930324]
11. Aksentijevich I, Putnam CD, Remmers EF, Mueller JL, Le J, Kolodner RD, et al. The clinical continuum of cryopyrinopathies: novel CIAS1 mutations in North American patients and a new cryopyrin model. *Arthritis Rheum.* 2007; 56:1273–85. [PubMed: 17393462]
12. Matsubayashi T, Sugiura H, Arai T, Oh-Ishi T, Inamo Y. Anakinra therapy for CINCA syndrome with a novel mutation in exon 4 of the CIAS1 gene. *Acta Paediatr.* 2006; 95:246–9. [PubMed: 16449034]
13. Jesus AA, Silva CA, Segundo GR, Aksentijevich I, Fujihira E, Watanabe M, et al. Phenotype–genotype analysis of cryopyrin-associated periodic syndromes (CAPS): description of a rare non-exon 3 and a novel CIAS1 missense mutation. *J Clin Immunol.* 2008; 28:134–8. [PubMed: 18080732]
14. Saito M, Fujisawa A, Nishikomori R, Kambe N, Nakata-Hizume M, Yoshimoto M, et al. Somatic mosaicism of CIAS1 in a patient with chronic infantile neurologic, cutaneous, articular syndrome. *Arthritis Rheum.* 2005; 52:3579–85. [PubMed: 16255047]
15. Erickson RP. Somatic gene mutation and human disease other than cancer: an update. *Mutat Res.* 2010; 705:96–106. [PubMed: 20399892]
16. Anderson JP, Mueller JL, Misaghi A, Anderson S, Sivagnanam M, Kolodner RD, et al. Initial description of the human NLRP3 promoter. *Genes Immun.* 2008; 9:721–6. [PubMed: 18719602]

**Figure 1.**

In vitro functional assessment of the identified *NLRP3* mosaicism mutations. **A**, Necrotic cell death of THP-1 cells induced by the identified somatic *NLRP3* mosaicism mutations. Green fluorescent protein (GFP)-fused mutant *NLRP3* was transfected into THP-1 cells. The percentage of dead cells (7-aminoactinomycin D positive) among GFP-positive cells is shown. Values are the mean  $\pm$  SD of triplicate experiments, and data are representative of 2 independent experiments. None = nothing transfected; mock = vector without *NLRP3*; WT = wild-type *NLRP3*; R260W = *NLRP3* with p.R260W (frequent mutations in patients with cryopyrin-associated periodic syndromes). **B**, ASC-dependent NF- $\kappa$ B activation induced by the identified somatic *NLRP3* mosaicism mutations. HEK 293FT cells were cotransfected with WT or mutant *NLRP3* in the presence or absence of ASC. The induction of NF- $\kappa$ B is shown as the fold change compared with cells that were transfected with a control vector without ASC (set at 1). Values are the mean  $\pm$  SD of triplicate experiments, and data are representative of 2 independent experiments.

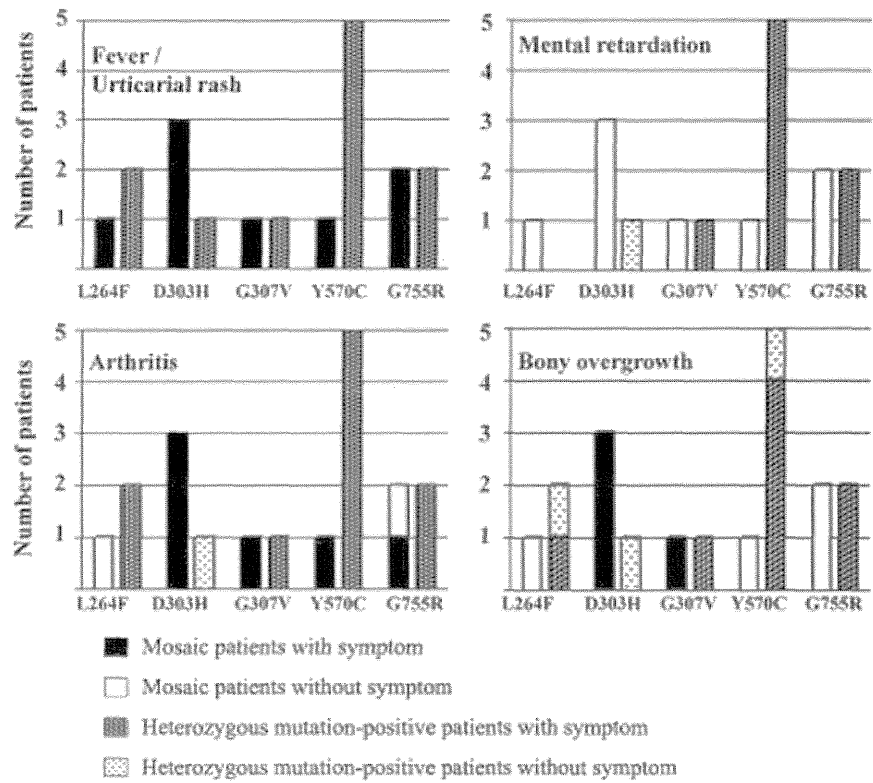


**Figure 2.**

Comparison of the clinical profiles of patients carrying somatic *NLRP3* mutations and patients carrying the same mutation, but with germline status. Clinical profiles of patients with mosaicism and those of patients with heterozygous germline mutations are compared for each protein variant (L264F, D303H, G307V, Y570C, and G755R). The data on 4 typical clinical symptoms are shown. Total numbers of patients with mosaicism and total numbers of patients with heterozygous mutation examined are shown as a bar for each protein variant. Each bar is stratified according to the presence or absence of the symptom. For the protein variant L264F, no data on mental retardation were available for the patient with a heterozygous germline mutation.

**Table 1**

Somatic mosaicism among mutation-negative NOMID/CINCA syndrome patients\*

Country, patient	Sequence variant	Protein variant	Mosaicism, %
France			
F1	1298C>T	T433I	5.2
F2	907G>C	D303H	4.2
F3	1315G>C	A439P	21.9
F4	1216A>G	M406V	9.2
F5	1698C>A	F566L	11.5
F6	None	–	–
Japan			
J1	1709A>G	Y570C	12.2
J2	790C>T	L264F	4.3
J3	919G>A	G307S	10.7
J4	1699G>A	E567K	6.5
J5	907G>C	D303H	11.9
J6	None	–	–
Spain			
S1	920G>T	G307V	9.6
S2	907G>C	D303H	19.1
S3	None	–	–
S4	None	–	–
US			
A1	1065A>T	K355N	18.8
A2	1698C>A	F566L	14.6
A3	1704G>C	K568N	9.4
A4	2263G>A	G755R	35.8
A5	None	–	–
A6	None	–	–
The Netherlands			
N1	1699G>A	E567K	6.3
N2	2263G>A	G755R	6.3
N3	None	–	–
N4	None	–	–

\* *NLRP3* mosaicism was detected in 18 of 26 patients (69.2%) with neonatal-onset multisystem inflammatory disease (NOMID)/chronic infantile neurologic, cutaneous, articular syndrome (CINCA syndrome). When samples from 19 healthy relatives of these patients were investigated, no somatic mosaicism was detected. The *P* value from the comparison of the cases and the controls (18 of 26 versus 0 of 19) was statistically significant ( $P < 0.0001$ ).

**Table 2**

Distribution and quantification of NLRP3 mutations among sources of genomic DNA (4 cell lineages and 1 tissue type) \*

Patient	Sequence variant	Protein variant	Mosaicism, %				
			Neutrophils	Monocytes	T cells	B cells	Buccal mucosa
J1	1709A>G	Y570C	12.6	9.8	8.0	9.5	8.3
J3	919G>A	G307S	9.1	10.8	6.9	10.6	9.0
J4	1699G>A	E567K	3.5	2.3	3.7	3.4	2.2
J5	907G>C	D303H	14.4	8.7	7.7	8.5	

\* No significant differences in the level of mosaicism were observed among the sources of genomic DNA.

**Table 3**

Clinical profiles of patients with somatic *NLRP3* mosaicism and patients with neither germline nor somatic *NLRP3* mutations \*

	Patients with somatic <i>NLRP3</i> mosaicism (n = 18)	Patients with neither germline nor somatic <i>NLRP3</i> mutations (n = 8)
Age, median (IQR) years	12 (1–30)	10 (3–21)
No. of men/women	10/8	3/5
Age at onset, median (IQR) months	0 (0–24)	0.5 (0–33)
Fever	17/17	7/7
Urticarial rash	14/14	8/8
Mental retardation	4/17	6/8
Meningitis	13/17	5/8
Seizures	2/18	1/7
Hearing loss	10/18	2/7
Arthritis	14/17	7/8
Bony overgrowth	12/17	6/7
Contractures	7/17	4/7
Walking disability	8/18	3/7
Biologic therapy	10/15	3/8

\* Except where indicated otherwise, values are the number with the feature/the total number of patients assessed. A lower incidence of mental retardation was observed in patients with somatic *NLRP3* mosaicism ( $P=0.03$ ). No other significant differences were detected between the groups. IQR = interquartile range.



## Rapid diagnosis of FHL3 by flow cytometric detection of intraplatelet Munc13-4 protein

Yuuki Murata,<sup>1</sup> Takahiro Yasumi,<sup>1</sup> Ryutaro Shirakawa,<sup>2</sup> Kazushi Izawa,<sup>1</sup> Hidemasa Sakai,<sup>1</sup> Junya Abe,<sup>1</sup> Naoko Tanaka,<sup>1</sup> Tomoki Kawai,<sup>1</sup> Koichi Oshima,<sup>3-5</sup> Megumu Saito,<sup>3</sup> Ryuta Nishikomori,<sup>1</sup> Osamu Ohara,<sup>4,5</sup> Eiichi Ishii,<sup>6</sup> Tatsutoshi Nakahata,<sup>3</sup> Hisanori Horiuchi,<sup>2</sup> and Toshio Heike<sup>1</sup>

<sup>1</sup>Department of Pediatrics, Kyoto University Graduate School of Medicine, Kyoto, Japan; <sup>2</sup>Department of Molecular and Cellular Biology, Institute of Development, Aging and Cancer, Tohoku University, Sendai, Japan; <sup>3</sup>Clinical Application Department, Center for iPS Cell Research and Application, Kyoto University, Kyoto, Japan; <sup>4</sup>Department of Human Genome Research, KAZUSA DNA Research Institute, Kisarazu, Japan; <sup>5</sup>Laboratory for Immunogenomics, Research Center for Allergy and Immunology, RIKEN, Yokohama, Japan; and <sup>6</sup>Department of Pediatrics, Ehime University Graduate School of Medicine, Toon, Japan

**Familial hemophagocytic lymphohistiocytosis (FHL) is a potentially lethal genetic disorder of immune dysregulation that requires prompt and accurate diagnosis to initiate life-saving immunosuppressive therapy and to prepare for hematopoietic stem cell transplantation. In the present study, 85 patients with hemophagocytic lymphohistiocytosis were screened for**

**FHL3 by Western blotting using platelets and by natural killer cell lysosomal exocytosis assay. Six of these patients were diagnosed with FHL3. In the acute disease phase requiring platelet transfusion, it was difficult to diagnose FHL3 by Western blot analysis or by lysosomal exocytosis assay. In contrast, the newly established flow cytometric analysis of**

**intraplatelet Munc13-4 protein expression revealed bimodal populations of normal and Munc13-4-deficient platelets. These findings indicate that flow cytometric detection of intraplatelet Munc13-4 protein is a sensitive and reliable method to rapidly screen for FHL3 with a very small amount of whole blood, even in the acute phase of the disease. (*Blood*. 2011;118(5):1225-1230)**

### Introduction

The granule-dependent cytotoxic pathway is a major immune effector mechanism used by cytotoxic T lymphocytes (CTLs) and natural killer (NK) cells.<sup>1</sup> The pathway involves a series of steps, including cell activation, polarization of the lysosomal granules to the immunologic synapse, exocytosis of lytic proteins such as perforin and granzymes, and induction of apoptosis in the target cells.<sup>2</sup> In addition to its central role in the defense against intracellular infections and in tumor immunity, this pathway also plays an important role in the regulation of immune homeostasis. Defects in the granule-dependent cytotoxic pathway result in a catastrophic hyperinflammatory condition known as hemophagocytic lymphohistiocytosis (HLH).<sup>1,3</sup>

HLH is a life-threatening syndrome of immune dysregulation resulting from the uncontrolled activation and proliferation of CTLs, which leads to macrophage activation and the excessive release of inflammatory cytokines.<sup>4,5</sup> Clinical diagnosis of HLH is made on the basis of cardinal signs and symptoms including prolonged fever and hepatosplenomegaly, and by characteristic laboratory findings such as pancytopenia, hyperferritinemia, hypofibrinogenemia, increased levels of soluble IL-2 receptor, and low or absent NK cell activity.<sup>5,6</sup> HLH can be classified into primary (genetic) or secondary (acquired) forms according to the underlying etiology, although this distinction is difficult to make in clinical practice.<sup>4,5</sup>

Familial hemophagocytic lymphohistiocytosis (FHL) encompasses major forms of primary HLH for which mutations in the genes encoding perforin (*PRF1*; FHL2),<sup>7</sup> Munc13-4

(*UNC13D*; FHL3),<sup>8</sup> syntaxin-11 (*STX11*; FHL4),<sup>9</sup> and syntaxin-binding protein 2 (also known as Munc18-2) (*STXB2*; FHL5)<sup>10,11</sup> have been identified to date. Perforin is a cytolytic effector that forms a pore-like structure in the target cell membrane. Munc13-4, syntaxin-11, and Munc18-2 are involved in intracellular trafficking or the fusion of cytolytic granules to the plasma membrane and the subsequent delivery of their contents into target cells.<sup>1,12</sup> Consequently, defective cytotoxic activity of CTLs and NK cells is one of the hallmark findings of FHL,<sup>7,8,13-16</sup> although NK cell activity is also decreased in some cases of secondary HLH.<sup>15,17-20</sup>

Prompt and accurate diagnosis of FHL is mandatory to initiate life-saving immunosuppressive therapy and to prepare for hematopoietic stem cell transplantation. Detection of perforin expression in NK cells with flow cytometry is a reliable method to screen for FHL2.<sup>21</sup> Another test analyzes the expression of CD107a on the surface of NK cells, which marks the release of cytolytic granules.<sup>22</sup> Reduced expression of CD107a implies impaired degranulation of NK cells and predicts a likelihood of FHL3.<sup>23</sup> However, this analysis is not available in some patients with extremely reduced NK cell numbers, such as during the acute phase of HLH.<sup>19</sup> In addition, NK-cell degranulation is also impaired in FHL4<sup>24</sup> and FHL5,<sup>10,11</sup> making it impossible to differentiate these disorders.

We reported previously that Munc13-4 protein is expressed in platelets and regulates the secretion of dense core granules.<sup>25</sup> Herein we report that Munc13-4 is expressed far more abundantly in platelets than in PBMCs. We also describe the development of a

Submitted January 10, 2011; accepted May 23, 2011. Prepublished online as *Blood* First Edition paper, June 8, 2011; DOI 10.1182/blood-2011-01-329540.

The online version of this article contains a data supplement.

The publication costs of this article were defrayed in part by page charge payment. Therefore, and solely to indicate this fact, this article is hereby marked "advertisement" in accordance with 18 USC section 1734.

© 2011 by The American Society of Hematology

new method to screen for FHL3 rapidly by detecting intraplatelet Munc13-4 expression through flow cytometry.

## Methods

### Patients

Between January 2008 and March 2010, whole blood samples from 85 patients were screened for FHL3. The patients had been clinically diagnosed with HLH by their referring physicians and were suspected of possible FHL. Characteristics of the enrolled patients are summarized in supplemental Table 1 (available on the *Blood* Web site; see the Supplemental Materials link at the top of the online article). As a control, blood obtained from healthy adults at the time of patient sampling was shipped for screening along with the patient samples. Before the laboratory studies were performed, informed consent was obtained from the patients and their parents, in accordance with the institutional review board of Kyoto University Hospital and the Declaration of Helsinki.

### Preparation of PBMCs and platelet samples

Whole blood samples treated with EDTA were centrifuged gently at 100g for 10 minutes, and platelets were collected from the supernatant plasma layer. Alternatively, platelets were prepared from small aliquots of blood samples by lysing red blood cells with ammonium chloride. PBMCs were obtained by Ficoll-Hypaque density gradient centrifugation from the remaining sample. CD4<sup>+</sup>, CD8<sup>+</sup>, CD14<sup>+</sup>, CD19<sup>+</sup>, and CD45<sup>+</sup> cells were separated from PBMCs using an AutoMACS Pro (Miltenyi Biotec) and magnetic bead-conjugated mAbs according to the manufacturer's instructions. Flow cytometric analysis revealed that each cell population contained > 95% CD4<sup>+</sup>, CD8<sup>+</sup>, CD14<sup>+</sup>, CD19<sup>+</sup>, and CD45<sup>+</sup> cells (data not shown).

### Mutation analysis

Genomic DNA was isolated from the PBMCs of patients with defective Munc13-4 expression using standard procedures. Primers were designed for the amplification and direct DNA sequencing of the *UNC13D*-coding exons, including the adjacent intronic sequences for the identification of splice-site variants. Primer sequences are available upon request. Products were sequenced directly with an ABI3130 genetic analyzer (Applied Biosystems).

### Antibodies

Rabbit polyclonal antibodies raised against the N-terminal region (residues 1-262)<sup>25</sup> and full-length human Munc13-4 protein were used as primary antibodies for Western blot and flow cytometric analysis, respectively. Rabbit polyclonal anti-integrin  $\alpha$ IIb (Santa Cruz Biotechnology) and mouse polyclonal anti- $\beta$ -actin (Sigma-Aldrich) antibodies were used as primary antibodies for Western blotting. The mAbs used in the flow cytometric analysis were FITC-conjugated anti-CD3 (SK7; BD Pharmingen), phycoerythrin (PE)-conjugated anti-CD41a (HIP8; BD Pharmingen), allophycocyanin-conjugated anti-CD56 (N901; Beckman Coulter), and PE-conjugated anti-CD107a (H4A3; eBioscience).

### Western blot analysis

Cell extracts were fractionated by SDS-PAGE, and the fractionated proteins were electrotransferred onto polyvinylidene fluoride membranes. The membranes were blocked overnight in blocking buffer (5% skim milk) and incubated for 1 hour at room temperature with the primary antibodies, followed by HRP-conjugated anti-rabbit or anti-mouse IgG polyclonal antibodies (Santa Cruz Biotechnology). Specific bands were visualized by the standard enhanced chemiluminescence method.

### Flow cytometric analysis of Munc13-4 protein

After surface staining with anti-CD41a mAbs, platelets were fixed and permeabilized by Cytofix/Cytoperm (BD Biosciences) and washed 3 times

with Perm/Wash buffer (BD Biosciences). After nonspecific reactions were blocked with Chrome-Pure human IgG (Jackson ImmunoResearch Laboratories), rabbit polyclonal antibody against the full-length human Munc13-4 protein was added, followed by FITC-conjugated donkey anti-rabbit IgG (Jackson ImmunoResearch Laboratories). Platelets were gated on the basis of their appearance on forward- and side-scatter plots in log/log scale and by CD41a expression. The gated platelets were analyzed for Munc13-4 expression by flow cytometry (FACSCalibur; BD Biosciences).

### Lysosomal degranulation assays

To quantify lysosome exocytosis by NK cells,  $2 \times 10^5$  PBMCs were mixed with  $2 \times 10^5$  human erythroleukemia cell line K562 cells and incubated for 2 hours in complete medium (RPMI 1640 medium supplemented with 2mM L-glutamine and 10% FCS) at 37°C in 5% CO<sub>2</sub>. Cells were resuspended in PBS supplemented with 2% FCS and 2mM EDTA; stained with anti-CD3-FITC, anti-CD56-allophycocyanin, and anti-CD107a-PE mAbs; and analyzed by flow cytometry.

Platelet exocytosis of the lysosomal granules was analyzed as described previously<sup>26</sup> but with a minor modification. Briefly, platelets were suspended in PBS containing 2mM EDTA and PE-conjugated anti-CD107a mAb, stimulated with 5 U/mL of thrombin (Wako Pure Chemical Industries) for 10 minutes at 25°C, and immediately analyzed by flow cytometry. The degranulation index of platelets was calculated as: (mean fluorescence value of stimulated sample – mean fluorescence value of nonstimulated sample)/mean fluorescence value of nonstimulated sample.

### Statistical analysis

Statistical analyses were performed with 1-way ANOVA followed by the Tukey post hoc test to compare multiple groups, with a  $P < .05$  level considered to be significant.

## Results

### Diagnosis of FHL3 by Western blot analysis using platelets

Before screening for FHL3, the Munc13-4 expression level was compared between platelets and PBMCs. Munc13-4 expression in platelets was approximately 10 times higher than that in PBMCs (Figure 1A). CD8<sup>+</sup> cells expressed a similar level of Munc13-4 protein as other PBMC cell types (Figure 1B). Similar amounts of platelet- and PBMC-derived proteins could be obtained from a sample (data not shown). Therefore, platelets were used to perform Western blotting to screen for Munc13-4 deficiency. Of the 85 patients screened, 6 patients were diagnosed with FHL3 (Figure 1C). Munc13-4 protein was barely detected in the platelets of each FHL3 patient regardless of the gene mutation (Table 1). For each sample, no more than 1 mL of whole blood was required to perform the analysis.

### Difficulty in diagnosing FHL3 in the acute phase of the disease

Patients in the acute phase of the disease who require screening for FHL often receive platelet transfusions because of thrombocytopenia.<sup>4,6</sup> To study the effect of transfused platelets on screening results, FHL3 screening was attempted in a patient receiving platelet transfusions. As expected, Western blotting using platelets could not detect Munc13-4 deficiency because of the normal expression of the protein in the transfused platelets (Figure 2A left column). Surprisingly, Western blotting using PBMCs also could not clearly identify Munc13-4 deficiency because a substantial number of platelets were present in the PBMCs obtained by the standard method (Figure 2A right column). By positively selecting CD45<sup>+</sup> cells and removing platelets, it was found that a considerable amount of the Munc13-4 protein detected in PBMC samples

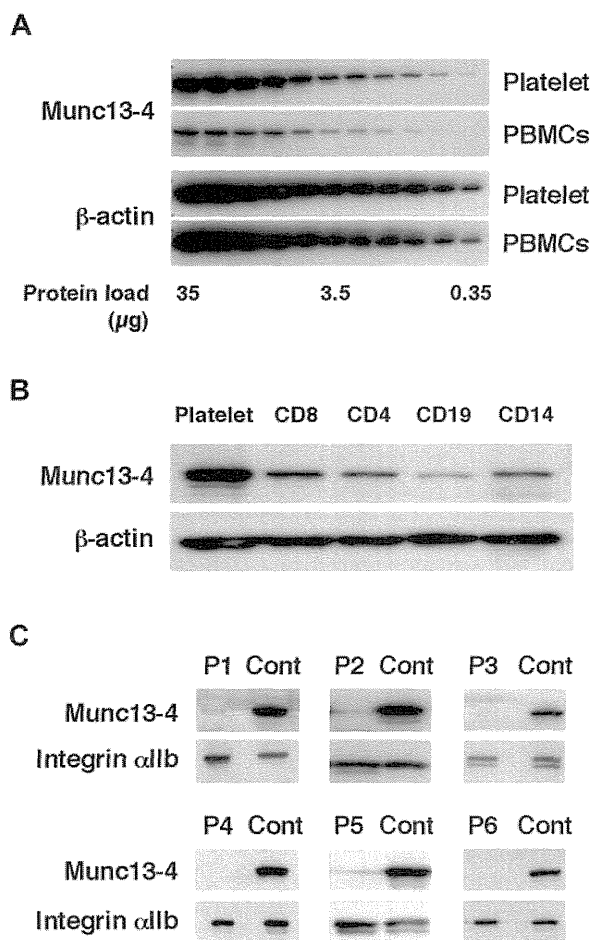


**Figure 1. Diagnosing FHL3 by Western blotting using platelet protein.** The amount of Munc13-4 protein expression was compared between platelets and PBMCs (A) and among platelets, CD8<sup>+</sup>, CD4<sup>+</sup>, CD19<sup>+</sup>, and CD14<sup>+</sup> cells (B) by Western blotting. A representative result of 5 independent experiments is shown. (C) Six FHL3 patients were diagnosed by Western blotting for Munc13-4 protein using platelets.

obtained by standard density gradient centrifugation was actually derived from the contaminating platelets (Figure 2B).

We performed a NK-cell degranulation assay for every referred sample and found the assay to be defective for every FHL3 patient identified (data not shown). All of the other patients showed a

**Table 1. UNC13D gene mutations of FHL3 patients**

Patient	Age at onset	Gender	Mutation	Genotype	Predicted effect
P1	14 days	Female	c.1596 + 1G → C	Homo	Splice error
P2	2 months	Male	c.322-1G → A	Hetero	Splice error
			c.990G → C	Hetero	p.Q330H
			c.3193C → T	Hetero	p.R1065X
P3	12 months	Female	c.754-1G → C	Hetero	Splice error
			c.2485delC	Hetero	p.L829fs
P4	4 months	Female	c.754-1G → C	Hetero	Splice error
			c.1799C → T	Hetero	p.T600M
			c.1803C → A	Hetero	p.Y601X
P5	2 months	Female	c.754-1G → C	Hetero	Splice error
			c.1596 + 1G → C	Hetero	Splice error
P6	5 months	Male	ND	ND	ND

Mutations were checked for single nucleotide polymorphisms using the dbSNP Build 132 database from the National Center for Biotechnology Information. X indicates stop; fs, frame shift; and ND, not determined.

normal release of lysosomal granules by NK cells; however, the analysis could not be performed in some patients because of the extremely low NK-cell number during the acute phase of the disease (data not shown).

We also examined the lysosomal granule release of platelets in 31 patients to determine whether this assay could be used as a screening method for FHL3. Lysosomal exocytosis of FHL3 platelets was partially impaired at steady state, but profound impairment was observed during the acute phase of the disease (Figure 3A-C). This profound impairment was also observed in platelets obtained from some secondary HLH patients during the acute phase (Figure 3B-C). These results indicate that it is difficult to diagnose FHL3 during the acute phase of HLH either by Western blot or by lysosomal degranulation assay.

**Rapid diagnosis of FHL3 by flow cytometric detection of intraplatelet Munc13-4**

To overcome the difficulty in diagnosing FHL3 during the acute phase of HLH, antibodies were raised against the full-length human Munc13-4 protein (supplemental Figure 1) and a new method was developed to detect Munc13-4 protein in platelets by flow cytometry. A total of 35 patients, including 4 with FHL3 (P3-P6), were

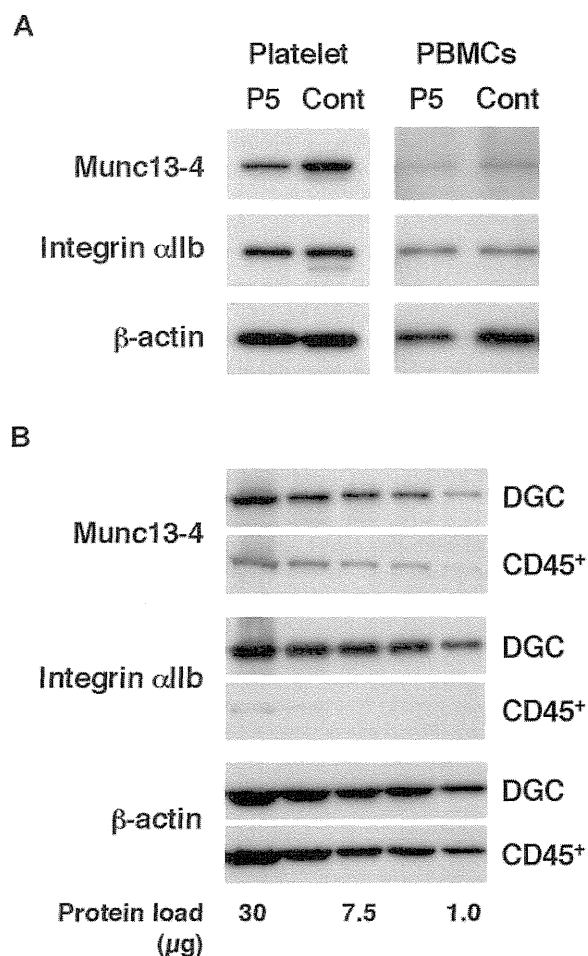


**Figure 2. Effect of platelet transfusion on Western blot analysis.** (A) Western blotting analysis for Munc13-4 expression using platelets and PBMCs from an FHL3 patient (P5) receiving platelet transfusions during the acute phase of the disease. (B) The expression of Munc13-4 was compared between PBMCs obtained by density gradient centrifugation (DGC) and CD45<sup>+</sup> cells obtained by magnetic sorting from healthy controls. A representative result of 3 independent experiments is shown.

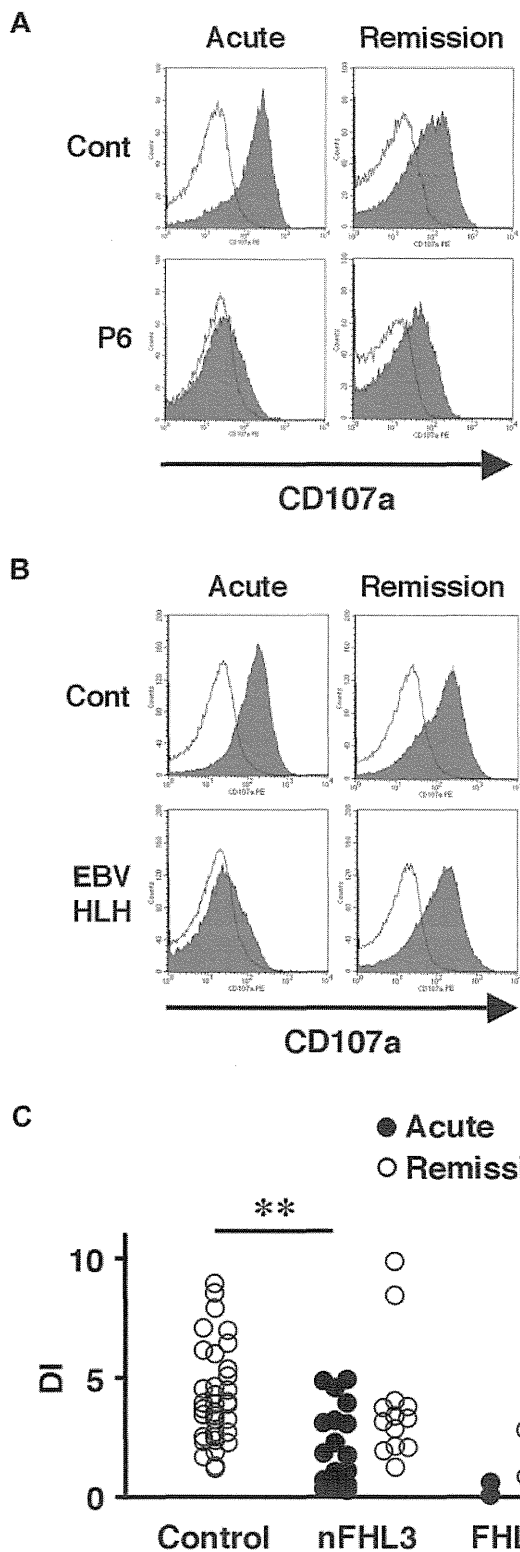


**Figure 3. Analysis of lysosomal exocytosis using platelets from HLH patients.** Platelets from an FHL3 patient (P6; A) and from a secondary (EBV-associated) HLH patient (B) along with healthy controls were left untreated (open histogram) or were stimulated with thrombin (closed histograms), and the surface expression of CD107a was analyzed by flow cytometry. Analysis was performed during the acute phase of the disease (left column) and after clinical remission (right column). (C) Degranulation index (DI) of platelets from HLH patients during the acute phase (●) and after clinical remission (○). HLH patients with normal NK-cell degranulation and Munc13-4 protein expression by Western blot analysis were defined as non-FHL3 (nFHL3). \*\**P* < .01 by the Tukey post hoc test.

analyzed using this method. Munc13-4 deficiency was readily detected in all of the FHL3 patients, with a sample volume of < 100 μL of whole blood (Figure 4A-C). Munc13-4 protein was expressed at normal level in the platelets of parents and siblings of FHL3 patients carrying heterozygous *UNC13D* mutations (data not shown). In the FHL3 patient receiving platelet transfusions, flow cytometric analysis revealed bimodal populations of normal and Munc13-4-deficient platelets (P5 in Figure 4A). As shown in Figure 4B, the method was able to clearly identify Munc13-4-deficient platelets in whole blood samples stored at room temperature for 1 week.

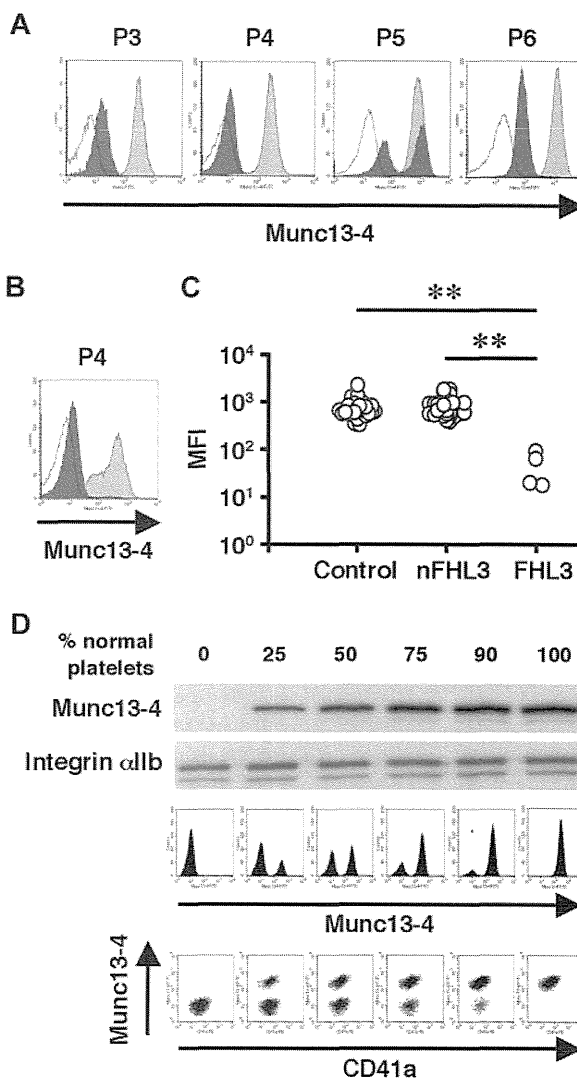


**Figure 4. Flow cytometric detection of intraplatelet Munc13-4 protein.** Flow cytometric analysis of intraplatelet Munc13-4 expression in 4 FHL3 patients and healthy controls using whole blood samples shipped overnight (A) and in an FHL3 patient (P4) and a healthy control using samples stored at room temperature for a week (B). Dark closed histograms represent platelets from FHL3 patients, whereas light closed histograms represent platelets from healthy controls. Open histograms represent staining with isotype controls. (C) Mean fluorescence intensity (MFI) of intraplatelet Munc13-4 staining for HLH patients and healthy controls. All of the healthy controls (*n* = 35) were adults. Non-FHL3 (nFHL3) patients (*n* = 31), as defined in Figure 3, varied in age (2 days-39 years) and included 2 patients with FHL2. Age-related variations in the MFI of Munc13-4 staining were not observed. \*\**P* < .01 by the Tukey post hoc test. (D) The sensitivities of Western blot and flow cytometric analyses for detecting Munc13-4-deficient platelets were compared.